Novel Zinc Oxide Nanostructures Produce by Hydrothermal Method Using different Reactors

Mohanad Q. Fahem[1*], Thamir A.A. Hassan[2]

Abstract

Zinc oxide (ZnO) nanoparticles were prepared with different structures and morphology by using the hydrothermal method. Multi-shape of reactor autoclaves (hom made) with different diminutions has been used. However, increasing the diameter of the autoclave led to slightly reducing the particles size of ZnO NPs. Therefore, the FESEM images show the semi-hexagonal shape with the big diameter of autoclaves and various shapes depending on the diameter of the autoclave. The energy dispersive spectroscopy (EDS) was appeared the atomic percentage of ZnO NPs decreases with Increase the diameter of the reactor. XRD patterns confirm the structure of ZnO NPs. Raman spectroscopy appeared broad peak at prepare with the smallest diameter and was showing high crystallization of nanostructure and red shifting when increasing the diameter of the autoclave.

Key Words: Hydrothermal, Raman Spectroscopy, ZnO, Novel Structure, Autoclave.

DOI Number: 10.14704/nq.2022.20.5.NQ22190 **NeuroQuantology 2022; 20(5):419-426**

Introduction

Zinc oxide (ZnO) nanostructure has been demonstrated to have numerous applications in recent years. Nanoscale materials offer a wide range of uses in various domains such as industry, health, environment, and medicine (Dhawale and Lokhande 2011; Rashid, Nayef, and Jabir 2021; Shinde, Gujar, and Lokhande 2007; Rashid, Nayef, and Jabir 2022; Y. Zhang and Mu 2007), as well as other applications such as optoelectronics, microelectronics, sensors, and transducers, due to their small size. Zinc oxide (ZnO) nanostructure has been demonstrated to have numerous applications in recent years. The semiconductor group II-VI includes ZnO. Due to its outstanding array of physical and optical features, such as the energy gap (3.37 eV) at ambient temperature and the high excitation binding energy (60 MeV), ZnO has attracted a lot of attention (Rashid, Nayef, and Jabir 2021; Lupan et al. 2007). It is abundant and provides a research arena for interpreting and comprehending one-dimensional nanostructures and their potential applications (Lupan et al. 2009) (Chai et al. 2011). Controlled synthesis and characterization of ZnO nanostructures are currently the focus of considerable attention. Hydrothermal synthesis (Hassan, Ali, and Qassim 2015; Wang et al. 2006; Sun et al. 2006; X.Y. Zhang et al. 2004)], vapour-liquid-solid (VLS) and vapor-solid (VS) processes (Yi, Wang, and Park 2005), Metal-Organic Chemical Vapor Deposition (MOCVD) (Galoppini et al. 2006), chemical vapor deposition (Yao and Yu 2007), and solution-liquid-solid growth in organic solvents (Li et al. 2000) (Hsu et al. 2005) (Park, Kim, and Han 2007). Have all been used to make ZnO nanostructures such as (nanosticks, nanotubes, nanowires, and nanobelts).

Corresponding author: Mohanad Q. Fahem

Address: [1*]Department of Physics, College of Science, University of Baghdad, Baghdad, Iraq; [2]Alkarkh University of Science, Baghdad, Iraq.

[1*]E-mail: mohand.qasem@gmail.com

Relevant conflicts of interest/financial disclosures: The authors declare that the research was conducted in the absence of any commercial or financial relationships that could be construed as a potential conflict of interest.

Received: 18 March 2022 **Accepted:** 23 April 2022

One-dimensional ZnO (1D) materials and ZnO nanocrystals of various forms have recently attracted a lot of attention due to their unique features, which are highly dependent on their size and shape, as well as their potential future usage as building blocks in nanodevices (X.Y. Zhang et al. 2004). ZnO nanocrystals in two and three dimensions will be crucial as novel functional units for electrical, electromechanical, and optoelectronic devices (Johnson et al. 2001) (Law and Thong 2006) (Hauschild and Kalt 2006) as well as nanosensors (Hassan, Ali, and Qassim 2015) (Wang et al. 2006) (Huang et al. 2001). Cells and chemical sensing applications are in the works right now. The goal of recent research has been to develop lightweight and flexible nanodevices (Galoppini et al. 2006) (Newton, Firth, and Warburton 2006).

In this study, ZnO NPs were prepared by the hydrothermal method depending on different volumetric autoclaves. The effect of autoclave diameter on the shape and particle size was studied; also the behavior of ZnO nanoparticles annealed with 363 k was investigated.

Experimental Part

1. Materiel and Methods

Zinc oxide (ZnO) Nano powder was purchased from (Tecnan-Spain) with purity 99.983 %; particle size 20-30 nm. NaOH was purchased from Sigma Aldrich with purity 98 % by using the hydrothermal method.

2. Setup the different Autoclave Reactors

Three stainless steel reactors (Z14, Z15 and Z16) of 100ml capacity with dimensions (diameter: height): Z14 (55mm: 130mm), Z15 (65mm: 100mm) and Z16 (75mm: 80mm) were designed and fabricated in our laboratory. Each reactor is composed of an inner Teflon autoclave positioned inside a stainless steel cylinder that can be tightly closed with a cylindrical cover. The cylinder acts as a furnace as it is surrounded externally by a heater of 3000W power an electric part for temperature control is at ached. The fabricated reactor parts are shown in Figure 1.

3. Preparation of ZnO NPs by Hydrothermal Method

One gram of ZnO nano-powder was added to 20ml of 3M NaOH at room temperature with continuous stirring until its colour changed to white (required time 20 minutes at the most). The suspension was put inside each autoclave reactor and heated to a temperature of 363k for 24 h. The product of the reaction from each reactor as washed several times with distilled water, dried for 30 min and filtered by Büchner funnel (with pore size=200nm). Furthermore, the product was heated at 523k for 1h for homogeneity and to remove any residual organic materials.

Structural properties of the prepared samples were studied by X-ray diffraction analysis, Raman spectroscopy, field emission scanning electron microscopy and energy-dispersive X-ray spectroscopy.

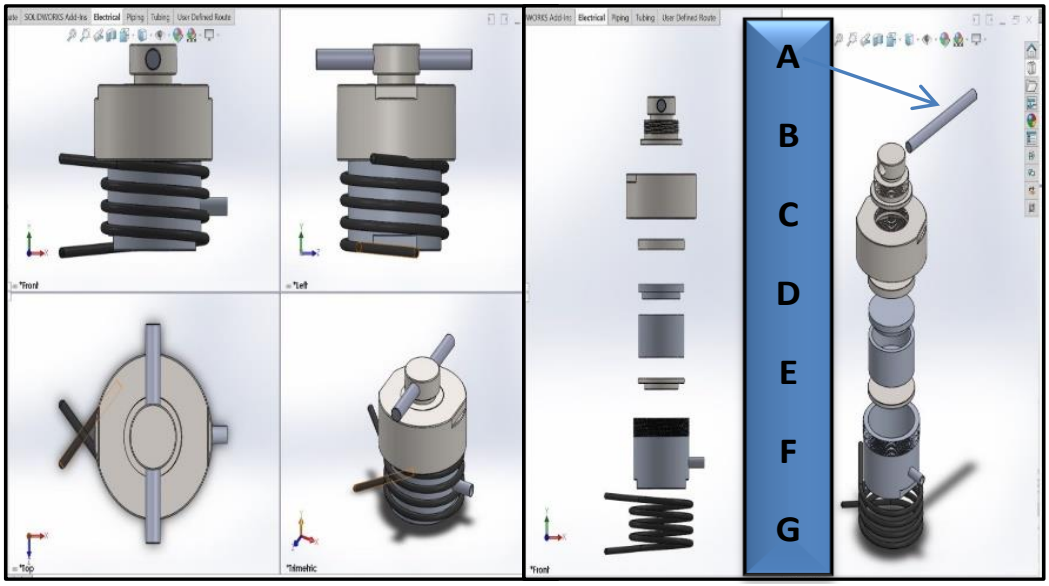

Fig. 1. The parts of the stainless steel autoclave (homemade), A: SS Grip the pole, B, C: Stainless steel lid, D, E: Gasket seal, F: Inside liner (Teflon autoclave), G: Lower Gasket seal, H: SS autoclave body and K: heater

Result and Discussions

Figure 2 shows the XRD patterns, recorded in the range of 20–80°, of the ZnO nanostructures prepared in the three reactors (Z14, Z15 and Z16) of different dimensions. The patterns show the strongest detected (h k l) of major peaks at 2θ values of 31.79°, 34.45°, 36.26°, 56.61°, 47.56° and 62.86° corresponding to the lattice planes (1 0 0), (0 0 2), (1 0 1), (1 1 0), (1 0 2) and (1 0 3), respectively for reaction time 24 h. The data are in agreement with the card for ZnO (JCPDS 96-230-0114) the Joint Committee on Powder Diffraction Standards. From the diffraction patterns, it was obvious that the growth is dominated in these directions and these diffraction peaks can be assigned to the wurtzite hexagonal-shaped ZnO. All peaks shown on this figure were identified as belonging to this card, and no other crystallized phases are observed. The film patterns clearly show an over-expression of the (002) peak when compared to the theoretical pattern; a similar behavior was already observed by other authors.

It was noticed that the peaks of ZnO from Z16 reactor were of higher intensity than those from Z15 and Z14 reactors, this indicates that ZnO from this reactor (Z16) was more crystallized.

Sharp and narrow peaks indicate that the ZnO particles have a high degree of crystallinity and purity. As can be seen from Figure 2, the intensity of the XRD peaks of the as-prepared ZnO samples increases as the reactor diameter decreased. This is due to the presence of an energetic model. Although there is a very little percentage of ZnO particles in the sample prepared according to EDS analysis of sample Z16. Therefore, changing the surface area of a reactor can lead to the synthesis of relatively pure ZnO particles (Ramimoghadam, Hussein, and Taufiq-Yap 2012).

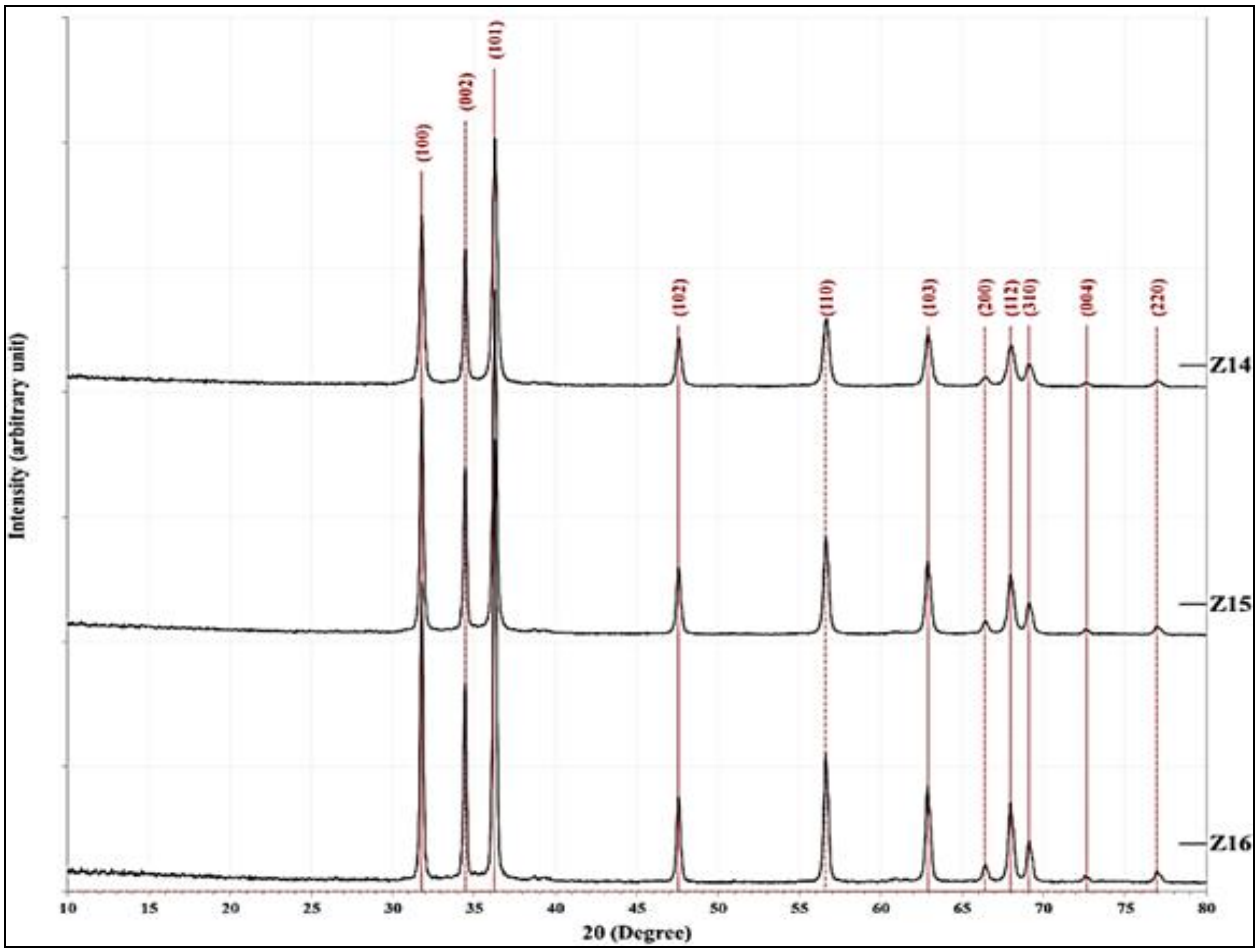

Fig. 2. XRD pattern for samples after restructured by the hydrothermal method at 363k for 24 h using different autoclave reactor (Z14), (Z15) and (Z16)

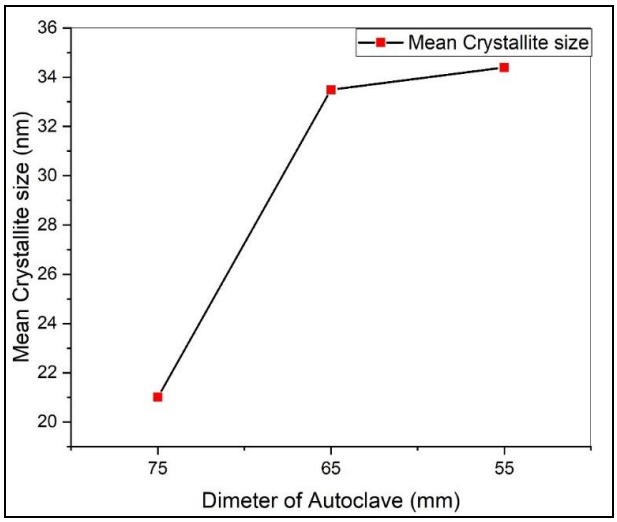

Fig. 3. The relation between mean crystallite size of ZnO NPs with Dimeter of Autoclave used

Figure 3 show the relation between the mean crystallite size of ZnO NPs with diameter of autoclave used. The crystallite size is decreased with diameter of autoclave increased, this phenomenon refer to the effect of surface area and this area maybe prevents aggregate of particles.

Table 1. Shows the allowed optical phonon modes in the Raman spectra of wurtzite ZnO using different autoclave reactors (Z14), (Z15) and (Z16)

Autoclave reactor	**Modes**	**Raman shift (cm^{-1})**
Z14	**E_2(low), B1(high)-B1(low), E1(TO), 2LO**	***66, 298, 405, 1122***
Z15	**E_2(low), B1(high)-B1(low)**	***66, 405***
Z16	**2TA; 2E2(low), TO+LO, TA+LO**	***147, 1050,669***

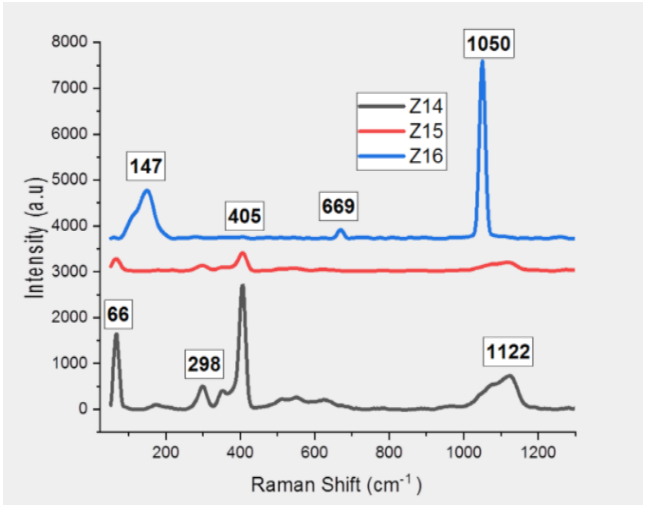

Fig. 4. Raman spectra for samples after restructured by hydrothermal at 363k for 24 h using different autoclave reactors (Z14), (Z15) and (Z16)

Micro-Raman scattering is a useful technique for determining the phase of low-dimensional pure nanostructures. In micro and nanostructures, the Raman spectrum is an important and adaptable diagnostic tool for studying crystallization, structural disorder, and flaws (Silambarasan, Saravanan, and Soga 2015). The characteristics of the as-prepared ZnO nanostructures from the three reactors were investigated using Micro-Raman spectroscopy. Graph 4. Wurtzite-type ZnO belongs to the space group C4 6v, and the primitive cell has two equivalent units. The irreducible representation can be used to classify photonic phonons at a position corresponding to the Brillouin region:

$$\Gamma_{opt} = A1 + E1 + 2E2 + 2B1$$

Both Raman and infrared active polar modes A1 and E1 are separated into transverse optical (TO) and longitudinal optical (LO) phonons. Only Raman activates E2 modes, which are non-polar. Raman and IR quiet modes are B1 modes (IR and Raman inactive). The non-polar modes of the second order, which is the only Raman active, are responsible for the lesser peak in the Raman spectrum. B1 modes and E2 (low) can clearly be observed in the recorded Raman spectra, showing that the radial structures have good crystal quality. The strength of retinal polar connections is reflected in both (TO) and (LO) (Bundesmann et al. 2003; Arguello, Rousseau, and Porto 1969; Xing 2003; Calleja and Cardona 1977; Damen, Porto, and Tell 1966; Montenegro et al. 2013).

Figure 4 shows which wurtzite ZnO phonons are observed by Raman scattering in the three reactors (as listed in Table 1). It is noted that the modes of the Raman spectrum of ZnO from Z15 reactor of E2(low), B1(high)-B1(low) are due to the imperfect crystal quality. A fairly strong polyphonic mode can be noted at the (2TA; 2E2 (low), TO+LO) modes because of the high crystallinity of the ZnO of the Z16 reactor. The Z14 reactor modes of the Raman spectrum E2(low), B1(high)-B1(low), E1(TO), 2LO. Figure 4 shows that the produced samples have a redshift; the displacement grows as the diameter of the reactor increases. The red shift is the polar opposite of the blue shift. The red shift indicates a decrease in the frequency of phonons interacting with the incident photon. The red-shift is caused by the material's improved crystallinity. Redshift occurs when material expands, resulting in a drop in frequency. In this research, the hydrothermal method was used, but we used a reactor of different dimensions, with the same conditions and size for

the hydrothermal process, and we got different results from one reactor to another. Previous research did not use such a procedure but rather worked on changing other variables other than the dimensions, but rather the size of the reactor. We did not change the size of the reactors. It is 100 ml. Conformation-controlled ZnO synthesis is of great importance for future ZnO nano device applications. Figure 5, shows elemental composition analyzes of ZnO NPs from the EDS plot of FE-SEM images. EDS spectra indicate that the required percentages of zinc are present in the percentage of zinc samples in the regions of samples Z14 and Z15, which gave strong Z16 more crystallized signals. Finally, we record observations of more crystallization taking place in the Z 16 sample, and this proves the XRD and FE-SEM results due to the different ratios of Zn, from energy dispersal X-ray spectroscopy (EDX), I found that the Zn:O ratios in our nanostructures It is a roughly stoichiometric ratio (1:1). The ZnO nanostructures may be seen in the FE-SEM pictures in Figure 5. When the diameter of the Z16 reactor is increased, a flower-like structure appears to grow, and when the reactor diameter is reduced, clusters of hexagonal crystals appear. A closer look at the flower-like structure reveals that it is made up of many nanoflakes and nanoparticles. The hexagonal rods generate a distinct spherical diagram of ZnO, and reducing the reactor diameter reduces the diameter and length of ZnO crystals [26]. The polarity and electrostatic attraction of ZnO nanoparticles cause this agglomeration (Fakhari, Jamzad, and Kabiri Fard 2019).

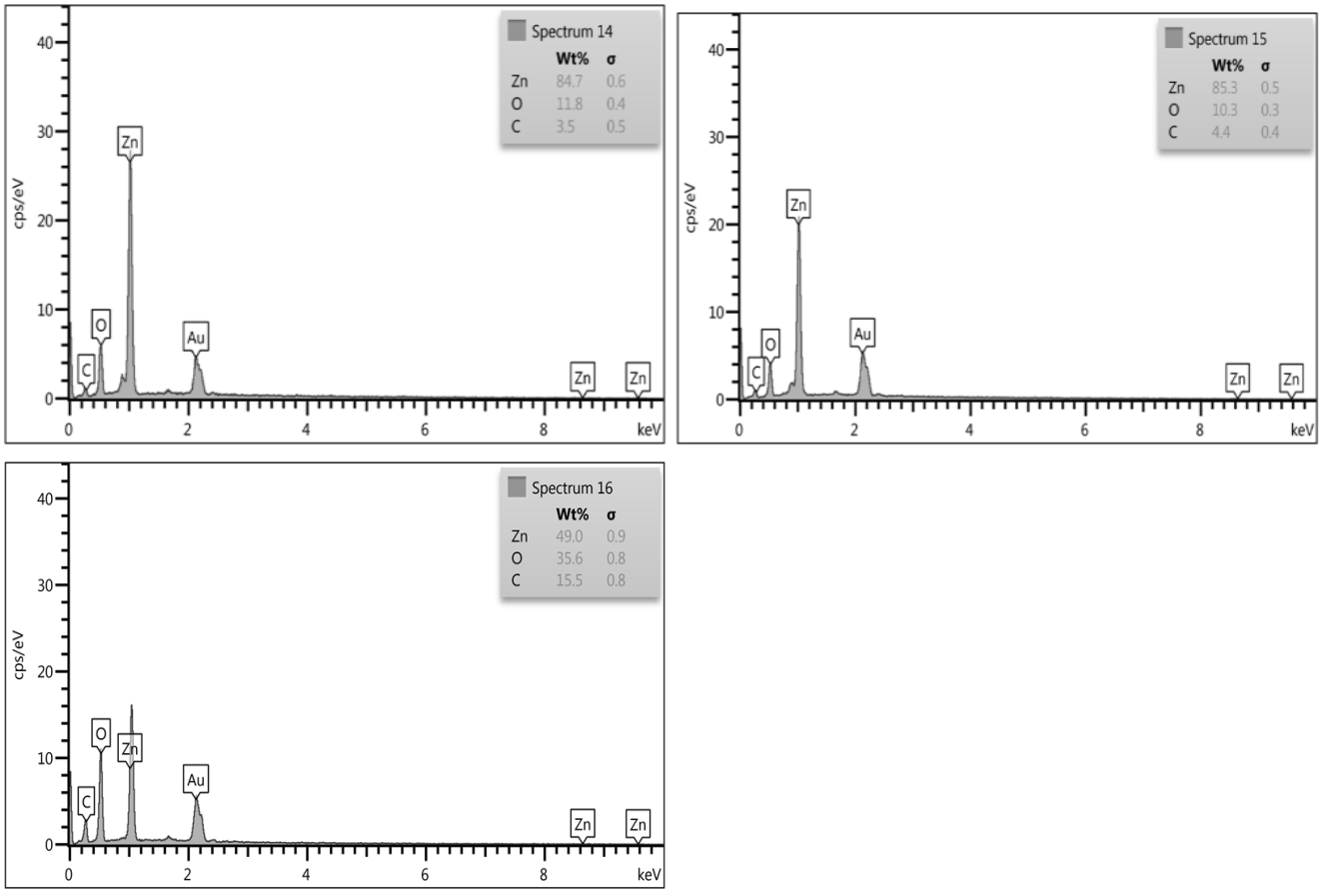

Fig. 5. EDS analyses of ZnO nanoparticles synthesized using different, autoclave reactors (Z14), (Z15) and (Z16).

Figure 6 shows elemental composition analyses of ZnO NPs based on the EDX plot of SEM images. The EDX spectra revealed that the samples contain the requisite phase of Zn and O, confirming the excellent purity of the produced ZnO NPs. The anticipated stoichiometric ratios of Zn:O for reactors Z14, Z15, and Z16 are 84.7 percent: 11.8 percent, 85.3 percent: 10.3, and 49 percent: 35.6 percent, respectively. For both produced nanoparticles, the EDX investigations in our study yielded similar results to those of prior studies (Fakhari, Jamzad, and Kabiri Fard 2019).

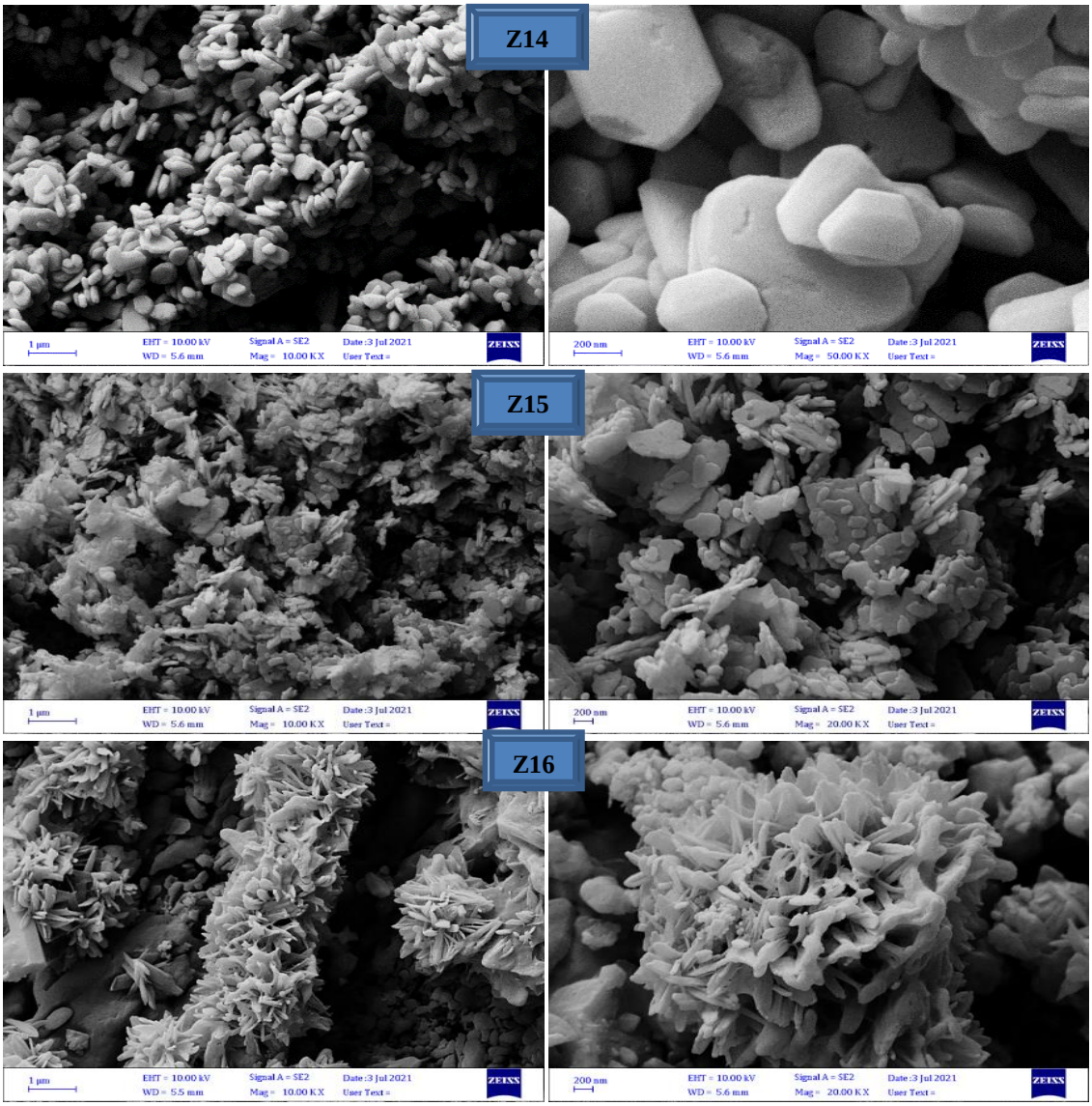

Fig. 6. The FE- SEM images of the ZnO nanostructured using different, autoclave reactors (Z14), (Z15) and (Z16)

Conclusion

This study was conducted using an environmentally friendly method, in which ZnO NPs were prepared by hydrothermal method using three different reactors with autoclave dimensions. The results showed that the effect of the difference in the surface area of the reactor with the same volume (100 ml) and under the same conditions differed in the results. The as-synthesized ZnO flowers are detailed in terms of their morphological, structural and optical properties by various analytical techniques such as FESEM, EDS, XRD and Raman measurements. The result of the XRD analysis showed an increase in the intensity of the XRD peaks of the ZnO samples prepared using the Z16 reactor with the increase in the diameter of the reactor, and this indicates the presence of high crystallinity of the prepared samples, and the XRD results confirmed the efficiency of preparing the samples using the hydrothermal method, and they grew in a very high density, and possessed a good hexagonal crystalline phase. The growing trend of the hydrothermal method shows a preference for the direction of strong growth of nanoflowers especially towards the reticular (101), (100) and (002) levels and confirming the hexagonal wurtzite structure. Despite the low percentage of zinc oxide that appeared in the EDS analysis. To examine the vibrational properties of the synthesized flower-shaped ZnO nanostructures, measurement of Raman scattering and high mode in Raman spectrum wurtzite confirm the hexagonal nature of the ZnO composite flowers and due to the presence of the active Raman mode, it can be concluded that the ZnO composite flowers possess a hexagonal phase with good crystal quality. As for the clear

transformation that appeared in the images of SEM analysis, where we notice a decrease in the crystal size with the increase in the diameter of the reactor, that is, with the increase in the surface area of the reactor, which gives the ability to maintain large electric fields. Responsible for creating flower-shaped structures using SEM.

References

Arguello, C.A., Denis L Rousseau, and S.P. da S Porto. 1969. "First-Order Raman Effect in Wurtzite-Type Crystals." *Physical Review,* 181(3): 1351.

Bundesmann, C, N Ashkenov, M Schubert, D Spemann, T Butz, EM Kaidashev, M Lorenz, and M Grundmann. 2003. "Raman Scattering in ZnO Thin Films Doped with Fe, Sb, Al, Ga, and Li." *Applied Physics Letters,* 83(10): 1974–76.

Calleja, J M, and Manuel Cardona. 1977. "Resonant Raman Scattering in ZnO." *Physical Review B,* 16(8): 3753.

Chai, G.Y., Lee Chow, Oleg Lupan, Emil Rusu, G.I. Stratan, Helge Heinrich, V.V. Ursaki, and I.M. Tiginyanu. 2011. "Fabrication and Characterization of an Individual ZnO Microwire-Based UV Photodetector." *Solid State Sciences,* 13(5): 1205–10.

Damen, T Co, SPS Porto, and B Tell. 1966. "Raman Effect in Zinc Oxide." *Physical Review,* 142(2): 570.

Dhawale, DS, and CD Lokhande. 2011. "Chemical Route to Synthesis of Mesoporous ZnO Thin Films and Their Liquefied Petroleum Gas Sensor Performance." *Journal of Alloys and Compounds,* 509(41): 10092–97.

Fakhari, Shabnam, Mina Jamzad, and Hassan Kabiri Fard. 2019. "Green Synthesis of Zinc Oxide Nanoparticles: A Comparison." *Green Chemistry Letters and Reviews,* 12(1): 19–24.

Galoppini, Elena, Jonathan Rochford, Hanhong Chen, Gaurav Saraf, Yicheng Lu, Anders Hagfeldt, and Gerrit Boschloo. 2006. "Fast Electron Transport in Metal Organic Vapor Deposition Grown Dye-Sensitized ZnO Nanorod Solar Cells." *The Journal of Physical Chemistry B,* 110(33): 16159–61.

Hassan, Thamir A A, Abdulkareem M Ali, and Ali Qassim. 2015. "Nano Rods and Flowerlike Synthesis by Hydrothermal Growth Method without Catalysts." *Engineering and Technology Journal,* 33(6 Part (B) Scientific).

Hauschild, Robert, and Heinz Kalt. 2006. "Guided Modes in ZnO Nanorods." *Applied Physics Letters,* 89 (12): 123107.

Hsu, Cheng-Liang, Shoou-Jinn Chang, Hui-Chuan Hung, Yan-Ru Lin, Chorng-Jye Huang, Yung-Kuan Tseng, and I-C Chen. 2005. "Vertical Single-Crystal ZnO Nanowires Grown on ZnO: Ga/Glass Templates." *IEEE Transactions on Nanotechnology,* 4(6): 649–54.

Huang, Michael H, Samuel Mao, Henning Feick, Haoquan Yan, Yiying Wu, Hannes Kind, Eicke Weber, Richard Russo, and Peidong Yang. 2001. "Room-Temperature Ultraviolet Nanowire Nanolasers." *Science,* 292 (5523): 1897–99.

Johnson, Justin C, Haoquan Yan, Richard D Schaller, Louis H Haber, Richard J Saykally, and Peidong Yang. 2001. "Single Nanowire Lasers." *The Journal of Physical Chemistry B,* 105(46): 11387–90.

Law, JBK, and JTL Thong. 2006. "Simple Fabrication of a ZnO Nanowire Photodetector with a Fast Photoresponse Time." *Applied Physics Letters,* 88(13): 133114.

Li, Y, GW Meng, LD Zhang, and F Phillipp. 2000. "Ordered Semiconductor ZnO Nanowire Arrays and Their Photoluminescence Properties." *Applied Physics Letters,* 76(15): 2011–13.

Lupan, Oleg, Lee Chow, Guangyu Chai, Beatriz Roldan, Ahmed Naitabdi, Alfons Schulte, and Helge Heinrich. 2007. "Nanofabrication and Characterization of ZnO Nanorod Arrays and Branched Microrods by Aqueous Solution Route and Rapid Thermal Processing." *Materials Science and Engineering: B,* 145(1–3): 57–66.

Lupan, Oleg, Lee Chow, S Shishiyanu, Eduard Monaico, T Shishiyanu, V Şontea, B Roldan Cuenya, Ahmed Naitabdi, Sanghoon Park, and A Schulte. 2009. "Nanostructured Zinc Oxide Films Synthesized by Successive Chemical Solution Deposition for Gas Sensor Applications." *Materials Research Bulletin,* 44(1): 63–69.

Montenegro, DN, V Hortelano, O Martínez, MC Martínez-Tomas, V Sallet, V Muñoz-Sanjosé, and J Jiménez. 2013. "Non-Radiative Recombination Centres in Catalyst-Free ZnO Nanorods Grown by Atmospheric-Metal Organic Chemical Vapour Deposition." *Journal of Physics D: Applied Physics,* 46(23): 235302.

Newton, Marcus C, Steven Firth, and Paul A Warburton. 2006. "ZnO Tetrapod Schottky Photodiodes." *Applied Physics Letters,* 89(7): 72104.

Park, Sun-Hong, Seon-Hyo Kim, and Sang-Wook Han. 2007. "Growth of Homoepitaxial ZnO Film on ZnO Nanorods and Light Emitting Diode Applications." *Nanotechnology,* 18(5): 55608.

Ramimoghadam, Donya, Mohd Zobir Bin Hussein, and Yun Hin Taufiq-Yap. 2012. "The Effect of Sodium Dodecyl Sulfate (SDS) and Cetyltrimethylammonium Bromide (CTAB) on the Properties of ZnO Synthesized by Hydrothermal Method." *International Journal of Molecular Sciences,* 13(10): 13275–93.

Rashid, Taha M, Uday M Nayef, and Majid S Jabir. 2021. "Nano-ZnO Decorated on Gold Nanoparticles as a Core-Shell via Pulse Laser Ablation in Liquid." *Optik,* 248: 168164.

"Synthesis of Au/ZnO Nanocomposite and Au: ZnO Core: Shell via Laser Ablation for of Photo-Catalytic Applications." *Materials Technology*, 1–8, 2022.

Shinde, VR, TP Gujar, and CD Lokhande. 2007. "LPG Sensing Properties of ZnO Films Prepared by Spray Pyrolysis Method: Effect of Molarity of Precursor Solution." *Sensors and Actuators B: Chemical,* 120(2): 551–59.

Silambarasan, M, S Saravanan, and T Soga. 2015. "Raman and Photoluminescence Studies of Ag and Fe-Doped ZnO Nanoparticles." *International Journal of ChemTech Research,* 7(3): 1644–50.

Sun, Ye, N George Ndifor-Angwafor, D Jason Riley, and Michael NR Ashfold. 2006. "Synthesis and Photoluminescence of Ultra-Thin ZnO Nanowire/Nanotube Arrays Formed by Hydrothermal Growth." *Chemical Physics Letters,* 431(4–6): 352–57.

Wang, JX, XW Sun, Y Yang, H Huang, YC Lee, OK Tan, and Lionel Vayssieres. 2006. "Hydrothermally Grown Oriented ZnO Nanorod Arrays for Gas Sensing Applications." *Nanotechnology,* 17(19): 4995.

Xing, YJ. 2003. "Xi ZH Xue ZQ Zhang XD Song JH Wang RM Appl." *Phys. Lett.,* 83: 1689.

Yao, Wei-Tang, and Shu-Hong Yu. 2007. "Recent Advances in Hydrothermal Syntheses of Low Dimensional

Nanoarchitectures." *International Journal of Nanotechnology,* 4 (1–2): 129–62.

Yi, Gyu-Chul, Chunrui Wang, and Won Il Park. 2005. "ZnO Nanorods: Synthesis, Characterization and Applications." *Semiconductor Science and Technology,* 20 (4): S22.

Zhang, XY, Ji Yan Dai, Hock Chun Ong, N Wang, HLW Chan, and CL Choy. 2004. "Hydrothermal Synthesis of Oriented ZnO Nanobelts and their Temperature Dependent Photoluminescence." *Chemical Physics Letters,* 393(1–3): 17–21.

Zhang, Yunyan, and Jin Mu. 2007. "Controllable Synthesis of Flower-and Rod-like ZnO Nanostructures by Simply Tuning the Ratio of Sodium Hydroxide to Zinc Acetate." *Nanotechnology,* 18 (7): 75606.